HHS Public Access

Author manuscript

Biochim Biophys Acta. Author manuscript; available in PMC 2016 July 01.

Published in final edited form as:

Biochim Biophys Acta. 2015 July ; 1848(7): 1536–1544. doi:10.1016/j.bbamem.2015.03.036.

Pore forming activity of the potent RTX-toxin produced by pediatric pathogen *Kingella kingae*: characterization and comparison to other RTX-family members*

Iván Bárcena-Uribarri[1], **Roland Benz**[1], **Mathias Winterhalter**[1], **Eleonora Zakharian**[2], and **Nataliya Balashova**[3]

[1]Department of Life Science and Chemistry, Jacobs University Bremen, Bremen, Germany

[2]Department of Cancer Biology & Pharmacology, University of Illinois College of Medicine at Peoria, Peoria, Illinois, USA

[3]Department of Pathology, School of Dental Medicine, University of Pennsylvania, Philadelphia, Pennsylvania, USA

Abstract

Pediatric septic arthritis in patients under age of four is frequently caused by the oral Gram-negative bacterium *Kingella kingae*. This organism may be responsible for a severe form of infective endocarditis in otherwise healthy children and adults. A major virulence factor of *K. kingae* is RtxA, a toxin that belongs to the RTX (Repeats-in-ToXin) group of secreted pore forming toxins. To understand the RtxA effects on host cell membranes, the toxin activity was studied using planar lipid bilayers. *K. kingae* strain PYKK081 and its isogenic RtxA-deficient strain, KKNB100, were tested for their ability to form pores in artificial membranes of asolectin/*n*-decane. RtxA, purified from PYKK081, was able to rapidly form pores with an apparent diameter of 1.9 nm as measured by the partition of nonelectrolytes in the pores. The RtxA channels are cation-selective and showed strong voltage-dependent gating. In contrast to supernatants of PYKK081, those of KKNB100 did not show any pore forming activity. We concluded that RtxA toxin is the only secreted protein from *K. kingae* forming large channels in host cell membranes where it induces cation flux leading to programmed cell death. Furthermore, our findings suggested that the planar lipid bilayer technique can effectively be used to test possible inhibitors of RTX toxin activity and to investigate the mechanism of the toxin binding to the membrane.

Keywords

RTX-toxins; bacterial pathogenesis; planar lipid bilayer

[#]Address correspondence to: Nataliya Balashova, Department of Pathology, University of Pennsylvania, School of Dental Medicine, 240 S. 40th St., 316 Levy Building, Philadelphia, PA 19104, USA. Tel.: (215) 898-5073; Fax: (215) 898-2050. natbal@dental.upenn.edu.

1. Introduction

Kingella kingae is a Gram-negative bacterium of the family *Neisseriaceae* and a normal component of human microflora that colonizes oral mucosal membranes of children [1]. Advances in approaches for microorganism's recovery from body fluids and the application of PCR methods for diagnostics in clinical labs have shown that *K. kingae* is a frequent cause of osteoarticular infections [2–8] and a common etiology of occult bacteremia [9] in children under 4 years of age. The organism is a part of the HACEK (*Haemophilus* species, *Aggregatibacter actinomycetemcomitans*, *Cardiobacterium hominis*, *Eikenella corrodens*, and *K. kingae*) group of oropharyngeal bacteria that share an enhanced capacity to produce endocardial infections [10]. *K. kingae* infective endocarditis is a severe infection [11–14] with an overall mortality rate of 16% [1]. Several outbreaks of invasive *K. kingae* infections in day care centers have been reported [15–17].

A principal virulence determinant of *K. kingae* is a 100 kDa protein toxin, RtxA, which belongs to the Repeats-in-ToXin (RTX) family [18]. RTX toxins are proteins secreted by type I export systems that destroy target cells by disrupting cell membranes [19]. Their protein structure contains a domain of glycine-rich nonapeptide calcium binding repeats, which are required for the toxin's activity [20, 21]. The toxins are activated by covalent fatty acid acylation of specific lysines, which represent a unique characteristic of this group of toxins [22–24].

The *rtxA* gene encoding RtxA has been found in all *K. kingae* clinical isolates and, hence, *rtxA* has been used as a specific biological marker to diagnose *K. kingae* infections [25–27]. In vitro studies using an RtxA deficient strain demonstrated that the toxin is solely responsible for cytotoxicity of *K. kingae* [18]. Our recent experimentation in an infant rat model has demonstrated that RtxA is the key virulence factor in this organism [28]. More specifically, RtxA affected animal immune system significantly by depleting white blood cells in the animals' blood and organs [28].

Earlier studies revealed a strong correlation between the lytic activity of RTX-toxins, CyaA and HlyA, on erythrocytes and macrophages with their pore forming activity in planar lipid bilayers [29–31]. The planar lipid bilayer assay is a highly sensitive method, which allows characterization of pores using small amounts of RTX-toxin samples. The present work is the first study to characterize the activity of *K. kingae* RtxA in planar lipid bilayers. Using the modulation of the conductance in the presence of small water soluble nonelectrolytes let us estimate the effective size of pores formed by RtxA. Thus, here we report the pore forming activity of *K. kingae* RtxA, and provide a biophysical characterization of the pores formed by the toxin in planar lipid membranes. Our results demonstrate the possibility to use planar lipid bilayers to investigate inhibitors of toxin activity and the binding mechanism to the membrane. This work also compares pores formed by different RTX toxins in planar lipid membranes.

2. Materials and methods

2.1. Bacterial strains and growth conditions

K. kingae strain PYKK081 producing RtxA was isolated in 1991 in Israel from the ankle joint of an 8 month old boy with septic arthritis. This strain was previously used in our studies [32] and its genome has been sequenced [33]. The RtxA-deficient strain KKNB100 was described elsewhere [28]. The bacteria were grown on Columbia agar (Oxoid LTD, Hampshire, England) with 5% sheep blood (Hemostat laboratories, Dixon, CA) at 37 °C with 10% CO_2 and were stored in AAGM broth [34] with 10% DMSO at −80 °C.

2.2. Purification of RtxA

Bacterial mass of *K. kingae* grown on Columbia agar with 5% sheep blood for 25 h, was collected, resuspended in 10 mM Tris-HCl, 20 mM NaCl pH 8.0, and incubated for 10 min at room temperature with shaking. Then, the suspension was centrifuged at 18,000 × g for 10 min to precipitate bacterial cells. The supernatant containing RtxA was collected and the protein was further purified from the filtered secreted fraction using a UnoQ cation-exchanger column (Bio-Rad, Hercules, CA). The proteins were eluted with a salt gradient 20 mM – 1 M NaCl using the Bio-Rad FPLC protein purification system (Bio-Rad, Hercules, CA). The toxin eluted as a fairly pure protein at 250 mM NaCl concentration.

2.3. SDS-PAGE and immunoassay

The protein samples were resolved by SDS-PAGE and visualized by silver nitrate staining [35] or transferred to nitrocellulose membranes. The membranes were subjected to Western blot analysis with 10A7D7 hybridoma supernatants (1:1000 dilution) containing an anti-RtxA monoclonal antibody [28] and the secondary HRP-Goat Anti-Mouse IgG (Fc) (1:10,000) (Pierce, Rockford, IL). If required, RtxA protein containing fractions were concentrated by centrifugation (18,000 × g, 10 min) using 10 K MWCO Centricon spin columns (Millipore, Billerica, MA). The protein concentration was estimated by BCA assay (Pierce, Rockford, IL).

2.4. Planar lipid bilayers

Single channel conductance—The planar lipid bilayer method has been described previously [36]. The membranes were formed from a 1% (w/v) solution of asolectin (phospholipids from soybean, Sigma-Aldrich) or diphytanoyl phosphatidylcholine (DiphPC, Avanti Polar Lipids, Alabaster, AL) in *n*-decane. The lipid membranes had a surface of approximately 0.5 mm^2 and they were formed using a Teflon loop to spread the lipid across the aperture in the dividing wall. After the membrane had turned black the toxin-containing protein fractions were added to the aqueous phase. The current across the membrane was measured with a pair of Ag/AgCl electrodes with salt bridges switched in series with a voltage source and a highly sensitive current amplifier Keithley 427 (Keithley Instruments, INC. Clevlend, OH). The signal was recorded by a strip chart recorder (Rikadenki Electronics GmbH, Freiburg, Germany). The temperature was kept at 20 °C throughout the experiment.

Ion selectivity—Zero-current membrane potential measurements were performed as described earlier [37]. The membranes were formed in 0.1 M salt solutions. A salt concentration gradient was gradually established across the membrane after toxin insertions reached a stationary phase by addition of 0.1 M salt solution to the trans-side (measuring electrode) and 3 M salt solution to the *cis*-side. The zero current membrane potential was measured once the electrochemical equilibrium was reached. Potentials were measured at the diluted side with a high impedance electrometer Keithley 617 (Keithley Instruments, INC. Clevlend, OH) and analyzed using the Goldman-Hodgkin-Katz equation [37].

The zero-current experiments were performed in KCl, LiCl, and KCH_3COO (KAc). The equivalent ionic conductivity at infinite dilution of the ions K^+, Cl^-, Li^+, and Ac^- were 70, 70, 40, and $39\times10^{-4}m^2Smol^{-1}$, respectively [38]. Based on these values it is assumed that the hydrodynamic radii of the pairs K/Cl and Li/Ac are equivalent.

Voltage-dependent gating—Voltage-dependent gating of the RTX toxins was studied as described elsewhere [39]. Briefly, after reconstitution of a large number of RtxA channels in a membrane, potentials in a range between −100 and +100 mV were applied. The membrane conductance (G) as a function of voltage (V_m) was measured immediately after applying the voltage and once again when the opening and closing of channels reached equilibrium. The conductance G at equilibrium was divided by the initial value of the conductance (G_o) obtained immediately after the onset of the voltage (which followed a linear function of the voltage) to analyze the gating of the channel.

Channel diameter estimation using nonelectrolytes—The determination of channel diameters using water soluble nonelectrolytes (NEs) has been previously described [40]. Small NEs penetrating a channel reduce its conductance due to an increase in the solution viscosity. The conductance of the RtxA toxin was measured in 1 M KCl solutions containing different NEs (20% w/v) with increasing hydrodynamic radii [40–42]. After the pore exclusion size is reached larger NEs cannot enter the channel and its interior is theoretically free of NEs. In these cases the conductance will be about the same as that measured in 1 M KCl solution free of NEs. Hence, the channel diameter should be approximately equal to the smallest NE that does not enter the channel and therefore does not reduce its conductance.

The size of a possible constriction inside the channel can be estimated using the channel filling concept. The filling of the channel (*F*) and its value in percentage (*F*%) were calculated as described elsewhere [40]. The filling (*F*) is given by:

$$F=[(G_0-G_i)/G_i]/[(X_0-X_i)/X_i] \quad \text{(eq. 1)}$$

where G_0 is the single-channel conductance in a solution without any NE (1 M KCl), G_i is the single-channel conductance in the presence of a solution containing 20% (w/v) of an NE. X_0 and X_i correspond to the conductivity of the salt solution without and with 20% (w/v) of a defined NE, respectively.

Assuming that the filling of the channel by two of the smallest NE (in our study ethylene glycol and glycerol) is close to the maximum possible level, the filling can be calculated in terms of percentage (*F%*):

$$F\%=2\cdot F_i/(F_1+F_2)\cdot 100\% \quad \text{(eq. 2)}$$

where F_i is the filling in the presence of a given NE and F_1 and F_2 represent filling in the presence of ethylene glycol and glycerol in the bathing solution respectively. The radius of the constriction zone should be equal to the radius of the smallest NE that does not pass freely through the channel and therefore does not fill it by 100%.

The following NEs were used: ethylene glycol, glycerol, arabinose, sorbitol (all obtained from Sigma-Aldrich; Munich, Germany), polyethylene glycol (PEG) 200, PEG 300, PEG 400, PEG 600, PEG 1000, PEG 2000, PEG 3350 and PEG 6000 (all obtained from Fluka; Munich, Germany). Polyethylene glycols were the molecules of choice in our studies because in aqueous solutions they have a spherical shape [43, 44]. At least 50 RtxA channels reconstituted into lipid membranes were analyzed to estimate the single channel conductance in the presence of the different NEs.

3. Results

3.1. Analysis of the pore forming activity of K. kingae supernatants

To study the pore forming capacity of *K. kingae* RtxA in the secreted fraction, we performed experiments with planar lipid bilayers. Toxin activity was tested using 50 to 100 μl (1 mg/ml of protein) of the supernatant of *K. kingae* PYKK081. The supernatants had a relatively low pore-forming activity in membranes formed of pure lipids, such as DiphPC/n-decane. Therefore, we switched to membranes formed of 1% asolectin/n-decane. The reason for this was the previous observation that HlyA from *E. coli* had a relatively small pore-forming activity in membranes from pure lipids but a very high activity in asolectin membranes [46]. Asolectin is composed of a heterogeneous mixture of lipids, mostly phosphatidylcholine (40%) as it is also the case in biological membranes. This lipid mixture facilitated channel formation by HlyA of *E. coli*, *Morganella morganii*, *Proteus vulgaris*, and also RtxA from *K. kingae* in the current study [45–48]. It is noteworthy, that no difference other than the channel-forming activity between the channels formed in membranes from DiphPC/n-decane and in membranes from asolectin/n-decane was observed. In 5–10 min after addition of the *K. kingae* supernatant to the aqueous solution bathing a black lipid bilayer membrane channel-formation was observed (see Fig. 1, left panel). This result was highly consistent and reproducible.

Besides supernatants of the RtxA producing strain PYKK081 we also used supernatants of the strain KKNB100, which is an isogenic RtxA-deficient strain [28]. These experiments were performed to investigate the possibility of the presence for other pore-forming proteins in the *K. kingae* supernatant and whether the pore observed in the supernatant of the strain PYKK081 could be RtxA. For these experiments we used the same experimental conditions as described above for the strain PYKK081. No pore-forming activity for more than 30 min was detected after adding up to 500 μl (1mg/ml of protein) of the strain KKNB100

supernatant (see Fig. 1, right panel). This result agrees with the assumption that no other pore forming component is present in supernatants of *K. kingae* strains and it also suggests that RtxA is solely responsible for the pore formation by the secreted fraction of strain PYKK081. This fact is consistent with our previous study where we found that strain KKNB100 did not produce any toxic effect on mammalian leukocytes [28].

3.2. Purification of RtxA from PYKK081

We attempted to further purify the secreted pore forming protein from PYKK081 using cation exchange chromatography. Two major protein peaks were detected: peak 1 (eluted with 125 mM NaCl) and peak 2 (eluted with 250 mM NaCl). The fractions from these peaks were collected and ten percent glycerol was added to the buffer to stabilize the toxin activity. While other contaminating proteins were found in the fractions of peak 1, the second peak contained only a 100 kDa protein band recognized by anti-RtxA antibody as RtxA (see Fig. 2A). The protein concentration in this fraction was 20 μg/ml. Thus, fractions from peak 2 were chosen to perform planar lipid bilayer experiments to study pore formation of RtxA.

3.3. Characterization of pore forming activity of purified RtxA in planar lipid bilayers

Purified RtxA was reconstituted in planar asolectin bilayers and channels were recorded in 1 M KCl at 20 mV applied membrane potential. Under these conditions RtxA formed channels with a conductance around 1.5 nS very similar to those formed by supernatants of the strain PYKK081 (see Fig. 2B). Fig. 2B also demonstrates that RtxA pores showed frequent channel gating despite a fairly homogeneous distribution of channels (see Fig. 2C).

Pore formation by RtxA was also measured in different KCl concentrations ranging from 0.01 to 3 M to gain more information about the properties of the open state of the channel. RtxA did not display a linear correlation between the salt concentration and the channel conductance similar to HlyA of *E. coli*. Instead, a dependence of the single channel conductance on the square root of the salt concentration was observed, which suggested that charges could interfere with transport of ions through the pore (see Table 1 and Fig. 7).

To study the channel selectivity, RtxA pore formation was also measured in 1 M LiCl and 1 M KAc (20 mV). Under these conditions the channel showed a single channel conductance of 0.7 and 1.3 nS respectively. In comparison to measurements in KCl, the replacement of K^+ by a less mobile cation, such as Li^+, has obviously a larger impact on pore conductance than replacing Cl^- by the less mobile anion acetate. This suggested that RtxA forms a channel with some preference for cations, i.e. it is a cation selective pore.

3.4. RtxA forms cation selective channels

To further evaluate the cation selectivity of RtxA toxin pores we performed zero membrane current experiments. To do that, after reconstitution of more than 10 pores in an asolectin membrane immersed in 0.1 M salt solution the concentration of the salts (KCl, LiCl or KAc) was increased five-fold on one side of the membrane (0.1 vs. 0.5 M). The asymmetry potential was measured at the diluted side of the membrane when it reached equilibrium. The KCl gradient resulted in an asymmetry potential of +19.9 mV (mean of 3

measurements) at the more dilute side of the membrane. A permeability ratio for K^+ over Cl^- (P_K/P_{Cl}) of 3.5 was calculated from the generated potential using the Goldman-Hodgkin-Katz equation (Table 2). This means that potassium ions contributed more preferentially to the conductance of the channel than chloride.

This result was confirmed by measurements with LiCl and potassium acetate. Under the same conditions as for KCl, we observed asymmetry potentials of 16.6 mV for LiCl and 21.0 mV for KAc at the more dilute side of the membrane for fivefold salt gradients. The corresponding ratios of cation permeability P_{cation} divided by anion permeability P_{anion} were 2.8 and 3.8, respectively (see Table 2). This suggested that size and/or mobility of cations and anions influenced the selectivity of the RtxA pore, which is in agreement with the situation observed previously for wide water-filled toxin channels, where size and hydration shell of the ions influence selectivity [29, 30, 45, 46]. These measurements suggested that the channel formed by RtxA of *K. kingae* is cation selective.

3.5. RtxA shows voltage-dependent gating

Membranes containing RtxA toxin channels from *K. kingae* were subjected to increasing positive and negative voltages to study its gating behavior. The RtxA pores were preferentially found in the open state at 20 mV applied voltage. However, already at this voltage some gating was also observed (see Figs. 1 and 2). A slight increase of the applied voltage (up to ±30–40 mV) in membranes containing pores formed by RtxA resulted in a drastic drop of the membrane conductance (to 40–60% of the original value). Thus, the RtxA pores seemed to be slightly more sensitive to negative voltages than to positive ones where gating started at lower voltages (see Fig. 3).

3.6. The RtxA pore has a radius of about 0.94 nm

The conductance of the RtxA pore was measured in presence of NEs, which allowed calculation of the size of the pore and also a rough estimate of a possible constriction inside the channel. The presence of the NEs in the aqueous solutions reduces their conductivity and the conductance of the channel if the neutral molecules have access to the channel interior. The conductance of the pore will increase to a value similar to one obtained in 1 M KCl if the NEs used were larger than the entrance of the pore. The size of the smallest NE that does not reduce the conductance of the channel can be considered similar in size to the entrance of the pore. In the case of RtxA from *K. kingae*, NEs with hydrodynamic radii between 0.26 and 0.8 nm reduced the conductance to 50–60 % of the one measured in 1M KCl. In NEs with bigger radii the conductance of the RtxA pore had values between 93 and 113 % of the conductance in absence of the NEs indicating no or highly reduced access of them to the channel interior (Table 3). Figure 4 shows the histograms of four representative measurements with the original channel insertions records embedded in panels. Figure 5 summarizes the ratios of the single channel conductance of RtxA in presence of the different NEs to that in the absence of any NE, i.e. in 1M KCl. The radius of the channel entrance can be then considered based in all this information to be close to the hydrodynamic radius of PEG 1000, i.e. it has a radius of about 0.94 nm.

A possible constriction of the pore can be estimated using the channel filling concept. The portion of the channel filled by the salt solution containing the different NEs can be calculated using Eqs. (1) and (2) given in the methods section. The radius of the channel constriction can be correlated to the radius of the smallest NE that does not fill the channel completely. In the case of RtxA non electrolytes with a radius smaller than 0.34 nm seem to fill the channel completely. NEs with radii between 0.39 and 0.80 nm exhibit similar channel filling values between 76 and 89 % excluding PEG 300 which seems to have a bigger deviation (Table 3). Figure 6 shows the dependence of F% on the hydrodynamic radii of the NEs. The radius of the entrance can be estimated from the intersection point between the horizontal line connecting NEs not filling the channel and the line connecting NEs which F% values are dependent on the NEs hydrodynamic radii. The radius of a possible constriction zone can be estimated from the radius of the smallest NE that does not fill the RtxA channel completely (F% lower than 100%). Figure 6 shows that the F% values of PEG 600 are very similar to the values obtained using glycerol The estimation of the channel filling showed in Eq. 2 is based on the assumption that glycerol fills the channel completely which suggest that PEG 600 could also be present along the entire channel. Taking this into account, the constriction of the channel should not be much narrower than the hydrodynamic radius of PEG 600, i.e the pore has a constriction with a radius of approx. 0.8 nm.

4. Discussion

Pore-forming toxins belonging to the RTX family have previously been found in a wide variety of Gram-negative bacteria including *E. coli* (HlyA), *Legionella* (RtxA), *Bordetella pertussis* (CyaA), *Proteus* (HlyA), *Morganella* (HlyA), *Vibrio cholera* (Rtx) and *Actinobacillus pleuropneumoniae* (ApxI, ApxII and ApXIII) [49–53]. These toxins form pores in cell membranes, which lose their function as barrier [54]. So far, some of these toxins have been studied using planar lipid bilayers [45, 46, 55–58] but the knowledge of the structure of these toxin pores is still limited.

RtxA showed enhanced activity in asolectin membranes similar as previously found for HlyA of *E. coli*, *M. morganii* and *P. vulgaris* [45, 46]. Nevertheless, the conductance of RtxA observed in DiphPC and asolectin was the same (around 1.5 nS in 1M KCl). Probably the composition of the membrane may influence insertion of this toxin but so far there is no indication that it influences its pore forming properties. Asolectin is a mixture of lipids from soy beans containing roughly equal proportions of phosphatidylcholine (PC, about 25%), phosphatidylethanolamine (PE), and phosphatidylinositol along with minor amounts other phospholipids and typical plant lipids, such as mono- and digalactosylglycerides. Interestingly, it has been previously shown that *A. actinomycetemcomitans* LtxA forms pores preferentially in liposomal membranes composed of lipids containing PE that is able to form inverted hexagonal (nonbilayer) phases in the bilayer membrane [59, 60]. It is also possible that specific hydrophobic interactions occur between the toxin and only certain phospholipids in asolectin membrane that are able to cause conformational changes necessary to facilitate the toxin binding to the membrane.

Both these possibilities could be a subject of further studies and could shed a light on the mechanism of RtxA specificity for cell membranes because the issue of the presence or absence of HlyA receptors on different cells is still controversial [61–64].

4.1. Single channel conductance and gating behavior of K. kingae RtxA pore

The RtxA toxin shows comparable channel conductance to those of general diffusion porins of Gram-negative bacteria [65]. However, the single channel conductance of the RTX toxins, including that of *K. kingae*, do not follow a linear function of the aqueous conductivity as it is usually the case for general diffusion porins [37, 65] (Table 1, Fig. 7). Furthermore, the pores fluctuated between open and closed states (Figs. 1 and 3). This means RtxA does not form a permanently open channel as it has been found for most Gram negative bacterial porins and some toxins [66, 67]. These results suggested that the RtxA pore of *K. kingae*, similar to other RTX toxins, does not represent a rigid structure and undergoes reversible structural changes as a function of applied voltage.

Haemolysin A (HlyA) of *E. coli* was first and the best studied RTX family member [31]. Single-channel recordings in planar lipid membranes demonstrated that HlyA forms cation selective channels with a conductance of about 500 pS in 0.15 M KCI [46]. RtxA from *K. kingae* shares a 46% homology of the primary sequence with HlyA and forms very similar pores in asolectin membranes based on the results described in this study (see Table 4).

All the RTX-toxins described until now are cation-selective (Table 4). In the case of the RtxA pore of *K. kingae* the zero-current membrane potentials for fivefold salt gradient concentration (0.1 vs. 0.5 M) were always positive regardless of the salt used (KCl, LiCl or KAc) and in a rage from 16 to 21 mV on the more dilute side. A similar behavior has also been observed for other RTX-toxins where the generated potentials were also positive even when the cations or anions where replaced by cations and anions (Li^+ and $KCH3COO^-$) of lower mobility in the aqueous phase [45, 46, 55–58]. This result suggested that cations preferentially penetrate the RTX channels and make a major contribution to channel conductance. In contrast to this, the selectivity of anion- or cation-selective general diffusion pores follow the mobility of the ions in the aqueous phase [37]. In the case of RtxA from *K. kingae* the cation selectivity seems to be somehow smaller as compared to that of other RTX toxins when the cation permeability P_{cation} divided by anion permeability P_{anion} are compared. *K. kingae* RtxA shows values of around 3.5 while most studied components of this family of toxins show values close to 10 (Table 4). For the discussion of this difference it has also been kept in mind that point net charges do not influence only the single-channel conductance but also the ion gradient across the channel, which may be smaller than the bulk aqueous gradient. This effect would result in a decrease of the apparent permeability ratio of cations over anions.

4.2. Size of the K. kingae RtxA channel

The channel diameter of different RTX toxins has been previously studied in detail using osmotic protection experiments or the mobility sequence for different cations within the channel [29, 31, 45, 46, 56, 57, 68]. Here, in addition to the single channel conductance, we studied the effect of nonelectrolytes on RtxA pore conductance. The conductance of the

toxin pores was investigated as a function of the hydrodynamic radii of different nonelectrolytes dissolved in the salt solution. These molecules have been used previously to determine the effective diameters of several channels reconstituted into planar lipid bilayers [40, 41, 69–71]. Inspection of the results from nonelectrolytes suggested that the RtxA pore has a diameter of around 1.9 nm. This pore size is in the range observed for other RTX toxins although it is somehow smaller compared to some RTX toxins with a very similar conductance as for example EHEC-HlyA [57], ApxI and ApxII [56] (see also Table 4). The channel diameter of HlyA from *E. coli* was estimated to be in a range from 1.4 to 3 nm [46, 68].

HlyA from *E. coli* and RtxA from *K. kingae* share a high homology in the primary amino acid sequence and very similar biophysical properties. The estimation of the pore diameter of both toxins using different methods is in agreement. Other RTX toxins with lower conductance like CyaA from *B. pertussis* displayed clearly smaller channels with a radius of about 0.8 nm [30].

4.3. Effect of point charges at the channel mouth

The single-channel conductance of *K. kingae* RtxA did not show a linear function of the salt concentration in the aqueous solution (Table 1). Instead, we observed its dependence on the square root of the aqueous salt concentration. This indicated firstly that the cation selectivity of the RtxA channel was not related to the presence of a binding site for ions and secondly that point charges at the channel mouth are involved in the ion selectivity as it has been previously shown for other RTX toxins [45, 46, 55, 56, 72] and also for cell wall porins of mycolata [73–75]. The effects of negatively charged amino acids at the channel mouth of the RtxA pore were studied as proposed by Menestrina and Antolini [76] for ion channels based on the model of Nelson and McQuarrie [77] about the ion distribution on membrane surfaces. The data displayed in Table 1 can be well fitted if we consider the channel to have a radius of 0.9 nm and 2.0 negative point charges ($q = -3.2 \cdot 10^{-19}$ As) attached to the channel mouth (Fig. 7). The solid line in Fig. 7 represents the fit of the single-channel conductance versus aqueous salt concentration by using the Nelson and McQuarrie treatment and the parameters mentioned above. The dashed line corresponds to the single-channel conductance of the RtxA pore with a slope of 1.5 nS/M without point net charges and shows a linear relationship between the aqueous salt concentration and the single-channel conductance of the toxin.

To sum up, *K. kingae* RtxA has similar pore forming properties as HlyA from *E. coli* and other RTX toxins as expected from the significant protein homology. The differences in single channel conductance, ion selectivity and channel diameter may however reflect some variations in the pore structures. Further protein structure analysis of these toxins will be required to determine the role of the polypeptide sequences and their respective folding in the activity and toxicity of each RTX pore forming toxin.

Acknowledgments

We are thankful to Pablo Yagupsky for providing *K. kingae* isolate PYKK081 and Joseph St. Geme III for sharing the mariner transposon system. The authors thank Edward T Lally and Angela Brown for the thoughtful discussion

of the results. This work was supported by BWF grant 1012758.01 (NB), DAAD grant A/13/09053 (NB) as well as the United States National Institute of Health grants R01DE009517 (Edward T Lally), and R01GM098052 (EZ).

References

1. Yagupsky P, Porsch E, St Geme JW 3rd. Kingella kingae: an emerging pathogen in young children. Pediatrics. 2011; 127:557–565. [PubMed: 21321033]
2. Yagupsky P, Dagan R, Prajgrod F, Merires M. Respiratory carriage of Kingella kingae among healthy children. The Pediatric infectious disease journal. 1995; 14:673–678. [PubMed: 8532424]
3. Yagupsky P, Dagan R, Howard CB, Einhorn M, Kassis I, Simu A. Clinical features and epidemiology of invasive Kingella kingae infections in southern Israel. Pediatrics. 1993; 92:800–804. [PubMed: 8233740]
4. Verdier I, Gayet-Ageron A, Ploton C, Taylor P, Benito Y, Freydiere AM, Chotel F, Berard J, Vanhems P, Vandenesch F. Contribution of a broad range polymerase chain reaction to the diagnosis of osteoarticular infections caused by Kingella kingae: description of twenty-four recent pediatric diagnoses. The Pediatric infectious disease journal. 2005; 24:692–696. [PubMed: 16094222]
5. Li X, Kolltveit KM, Tronstad L, Olsen I. Systemic diseases caused by oral infection. Clin Microbiol Rev. 2000; 13:547–558. [PubMed: 11023956]
6. Ilharreborde B, Bidet P, Lorrot M, Even J, Mariani-Kurkdjian P, Liguori S, Vitoux C, Lefevre Y, Doit C, Fitoussi F, Pennecot G, Bingen E, Mazda K, Bonacorsi S. New real-time PCR-based method for Kingella kingae DNA detection: application to samples collected from 89 children with acute arthritis. Journal of clinical microbiology. 2009; 47:1837–1841. [PubMed: 19369442]
7. Gene A, Garcia-Garcia JJ, Sala P, Sierra M, Huguet R. Enhanced culture detection of Kingella kingae, a pathogen of increasing clinical importance in pediatrics. The Pediatric infectious disease journal. 2004; 23:886–888. [PubMed: 15361737]
8. Chometon S, Benito Y, Chaker M, Boisset S, Ploton C, Berard J, Vandenesch F, Freydiere AM. Specific real-time polymerase chain reaction places Kingella kingae as the most common cause of osteoarticular infections in young children. The Pediatric infectious disease journal. 2007; 26:377–381. [PubMed: 17468645]
9. Dubnov-Raz G, Ephros M, Garty BZ, Schlesinger Y, Maayan-Metzger A, Hasson J, Kassis I, Schwartz-Harari O, Yagupsky P. Invasive pediatric Kingella kingae Infections: a nationwide collaborative study. Pediatr Infect Dis J. 2010; 29:639–643. [PubMed: 20182400]
10. Das M, Badley AD, Cockerill FR, Steckelberg JM, Wilson WR. Infective endocarditis caused by HACEK microorganisms. Annu Rev Med. 1997; 48:25–33. [PubMed: 9046942]
11. Rotstein A, Konstantinov IE, Penny DJ. Kingella-infective endocarditis resulting in a perforated aortic root abscess and fistulous connection between the sinus of Valsalva and the left atrium in a child. Cardiology in the young. 2010; 20:332–333. [PubMed: 20474102]
12. Lee WL, Dooling EC. Acute Kingella kingae endocarditis with recurrent cerebral emboli in a child with mitral prolapse. Ann Neurol. 1984; 16:88–89. [PubMed: 6465865]
13. Holmes AA, Hung T, Human DG, Campbell AI. Kingella kingae endocarditis: A rare case of mitral valve perforation. Ann Pediatr Cardiol. 2011; 4:210–212. [PubMed: 21976892]
14. Berkun Y, Brand A, Klar A, Halperin E, Hurvitz H. Kingella kingae endocarditis and sepsis in an infant. European journal of pediatrics. 2004; 163:687–688. [PubMed: 15300433]
15. Kiang KM, Ogunmodede F, Juni BA, Boxrud DJ, Glennen A, Bartkus JM, Cebelinski EA, Harriman K, Koop S, Faville R, Danila R, Lynfield R. Outbreak of osteomyelitis/septic arthritis caused by Kingella kingae among child care center attendees. Pediatrics. 2005; 116:e206–213. [PubMed: 16024681]
16. Sena AC, Seed P, Nicholson B, Joyce M, Cunningham CK. Kingella kingae endocarditis and a cluster investigation among daycare attendees. The Pediatric infectious disease journal. 2010; 29:86–88. [PubMed: 19884874]
17. Yagupsky P, Erlich Y, Ariela S, Trefler R, Porat N. Outbreak of Kingella kingae skeletal system infections in children in daycare. The Pediatric infectious disease journal. 2006; 25:526–532. [PubMed: 16732151]

18. Kehl-Fie TE, St Geme JW 3rd. Identification and characterization of an RTX toxin in the emerging pathogen Kingella kingae. Journal of bacteriology. 2007; 189:430–436. [PubMed: 17098895]
19. Linhartova I, Bumba L, Masin J, Basler M, Osicka R, Kamanova J, Prochazkova K, Adkins I, Hejnova-Holubova J, Sadilkova L, Morova J, Sebo P. RTX proteins: a highly diverse family secreted by a common mechanism. FEMS Microbiol Rev. 2010; 34:1076–1112. [PubMed: 20528947]
20. Goni FM, Ostolaza H. E. coli alpha-hemolysin: a membrane-active protein toxin. Braz J Med Biol Res. 1998; 31:1019–1034. [PubMed: 9777009]
21. Ostolaza H, Soloaga A, Goni FM. The binding of divalent cations to Escherichia coli alpha-haemolysin. European journal of biochemistry / FEBS. 1995; 228:39–44. [PubMed: 7883008]
22. Balashova NV, Shah C, Patel JK, Megalla S, Kachlany SC. Aggregatibacter actinomycetemcomitans LtxC is required for leukotoxin activity and initial interaction between toxin and host cells. Gene. 2009; 443:42–47. [PubMed: 19450669]
23. Stanley P, Koronakis V, Hughes C. Acylation of Escherichia coli hemolysin: a unique protein lipidation mechanism underlying toxin function. Microbiol Mol Biol Rev. 1998; 62:309–333. [PubMed: 9618444]
24. Stanley P, Packman LC, Koronakis V, Hughes C. Fatty acylation of two internal lysine residues required for the toxic activity of Escherichia coli hemolysin. Science. 1994; 266:1992–1996. [PubMed: 7801126]
25. Ceroni D, Cherkaoui A, Ferey S, Kaelin A, Schrenzel J. Kingella kingae osteoarticular infections in young children: clinical features and contribution of a new specific real-time PCR assay to the diagnosis. J Pediatr Orthop. 2010; 30:301–304. [PubMed: 20357599]
26. Cherkaoui A, Ceroni D, Emonet S, Lefevre Y, Schrenzel J. Molecular diagnosis of Kingella kingae osteoarticular infections by specific real-time PCR assay. Journal of medical microbiology. 2008; 58:65–68. [PubMed: 19074654]
27. Lehours P, Freydiere AM, Richer O, Burucoa C, Boisset S, Lanotte P, Prere MF, Ferroni A, Lafuente C, Vandenesch F, Megraud F, Menard A. The rtxA toxin gene of Kingella kingae: a pertinent target for molecular diagnosis of osteoarticular infections. J Clin Microbiol. 2011; 49:1245–1250. [PubMed: 21248099]
28. Chang DW, Nudell YA, Lau J, Zakharian E, Balashova NV. RTX Toxin Plays a Key Role in Kingella kingae Virulence in an Infant Rat Model. Infection and immunity. 2014; 82:2318–2328. [PubMed: 24664507]
29. Benz R, Maier E, Ladant D, Ullmann A, Sebo P. Adenylate cyclase toxin (CyaA) of Bordetella pertussis. Evidence for the formation of small ion-permeable channels and comparison with HlyA of Escherichia coli. The Journal of biological chemistry. 1994; 269:27231–27239. [PubMed: 7525549]
30. Masin J, Basler M, Knapp O, El-Azami-El-Idrissi M, Maier E, Konopasek I, Benz R, Leclerc C, Sebo P. Acylation of lysine 860 allows tight binding and cytotoxicity of Bordetella adenylate cyclase on CD11b-expressing cells. Biochemistry. 2005; 44:12759–12766. [PubMed: 16171390]
31. Menestrina G, Mackman N, Holland IB, Bhakdi S. Escherichia coli haemolysin forms voltage-dependent ion channels in lipid membranes. Biochimica et biophysica acta. 1987; 905:109–117. [PubMed: 2445378]
32. Maldonado R, Wei R, Kachlany SC, Kazi M, Balashova NV. Cytotoxic effects of Kingella kingae outer membrane vesicles on human cells. Microb Pathog. 2011; 51:22–30. [PubMed: 21443941]
33. Kaplan JB, Lo C, Xie G, Johnson SL, Chain PS, Donnelly R, Kachlany SC, Balashova NV. Genome Sequence of Kingella kingae Septic Arthritis Isolate PYKK081. J Bacteriol. 2012; 194:3017. [PubMed: 22582375]
34. Fine DH, Furgang D, Kaplan J, Charlesworth J, Figurski DH. Tenacious adhesion of Actinobacillus actinomycetemcomitans strain CU1000 to salivary-coated hydroxyapatite. Archives of oral biology. 1999; 44:1063–1076. [PubMed: 10669085]
35. Blum H, Beier H, Gross HJ. Improved silver staining of plant proteins, RNA and DNA in polyacrylamide gels. Electrophoresis. 1987; 8:93–99.

36. Benz R, Janko K, Boos W, Lauger P. Formation of large, ion-permeable membrane channels by the matrix protein (porin) of Escherichia coli. Biochimica et biophysica acta. 1978; 511:305–319. [PubMed: 356882]
37. Benz R, Janko K, Lauger P. Ionic selectivity of pores formed by the matrix protein (porin) of Escherichia coli. Biochimica et biophysica acta. 1979; 551:238–247. [PubMed: 369608]
38. Lide DR. CRC Handbook of Chemistry and Physics. :5–97. 95–98.
39. Ludwig O, De Pinto V, Palmieri F, Benz R. Pore formation by the mitochondrial porin of rat brain in lipid bilayer membranes. Biochimica et biophysica acta. 1986; 860:268–276. [PubMed: 2427116]
40. Krasilnikov OV, Da Cruz JB, Yuldasheva LN, Varanda WA, Nogueira RA. A novel approach to study the geometry of the water lumen of ion channels: colicin Ia channels in planar lipid bilayers. The Journal of membrane biology. 1998; 161:83–92. [PubMed: 9430623]
41. Krasilnikov OV, Sabirov RZ, Ternovsky VI, Merzliak PG, Muratkhodjaev JN. A simple method for the determination of the pore radius of ion channels in planar lipid bilayer membranes. FEMS microbiology immunology. 1992; 5:93–100. [PubMed: 1384601]
42. Sabirov RZ, Krasilnikov OV, Ternovsky VI, Merzliak PG. Relation between ionic channel conductance and conductivity of media containing different nonelectrolytes. A novel method of pore size determination. General physiology and biophysics. 1993; 12:95–111. [PubMed: 7691679]
43. Mark JE, Flory PJ. The configuration of the polyoxyethylene chain. J Am Chem Soc. 1965; 87:1415–1422.
44. Rempp PJ. Contribution a l'étude des solution de molecules en chain a squelette oxigène. Chem Phys. 1957; 54:432–453.
45. Benz R, Hardie KR, Hughes C. Pore formation in artificial membranes by the secreted hemolysins of Proteus vulgaris and Morganella morganii. European journal of biochemistry / FEBS. 1994; 220:339–347. [PubMed: 7510229]
46. Benz R, Schmid A, Wagner W, Goebel W. Pore formation by the Escherichia coli hemolysin: evidence for an association-dissociation equilibrium of the pore-forming aggregates. Infection and immunity. 1989; 57:887–895. [PubMed: 2465272]
47. Alberts JAB, Lewis J, Raff M, Roberts K, Walter P. The Lipid Bilayer. Molecular Biology of the Cell (4). 2002 Table 10–11.
48. Scholfield CR. Composition of Soybean Lecithin. Journal of the American Oil Chemists' Society. 1981; 58:889–892.
49. Cirillo SL, Bermudez LE, El-Etr SH, Duhamel GE, Cirillo JD. Legionella pneumophila entry gene rtxA is involved in virulence. Infection and immunity. 2001; 69:508–517. [PubMed: 11119544]
50. Glaser P, Sakamoto H, Bellalou J, Ullmann A, Danchin A. Secretion of cyclolysin, the calmodulin-sensitive adenylate cyclase-haemolysin bifunctional protein of Bordetella pertussis. The EMBO journal. 1988; 7:3997–4004. [PubMed: 2905265]
51. Lin W, Fullner KJ, Clayton R, Sexton JA, Rogers MB, Calia KE, Calderwood SB, Fraser C, Mekalanos JJ. Identification of a vibrio cholerae RTX toxin gene cluster that is tightly linked to the cholera toxin prophage. Proc Natl Acad Sci U S A. 1999; 96:1071–1076. [PubMed: 9927695]
52. Lo RY. Molecular characterization of cytotoxins produced by Haemophilus, Actinobacillus, Pasteurella. Canadian journal of veterinary research = Revue canadienne de recherche veterinaire. 1990; 54(Suppl):S33–35. [PubMed: 2193701]
53. Lovell R, Rees TA. A filterable haemolysin from Escherichia coli. Nature. 1960; 188:755–756. [PubMed: 13763779]
54. Iacovache I, van der Goot FG, Pernot L. Pore formation: an ancient yet complex form of attack. Biochimica et biophysica acta. 2008; 1778:1611–1623. [PubMed: 18298943]
55. Benz R, Maier E, Ladant D, Ullmann A, Sebo P. Adenylate cyclase toxin (CyaA) of Bordetella pertussis. Evidence for the formation of small ion-permeable channels and comparison with HlyA of Escherichia coli. The Journal of biological chemistry. 1994; 269:27231–27239. [PubMed: 7525549]

56. Maier E, Reinhard N, Benz R, Frey J. Channel-forming activity and channel size of the RTX toxins ApxI, ApxII, and ApxIII of Actinobacillus pleuropneumoniae. Infection and immunity. 1996; 64:4415–4423. [PubMed: 8890186]
57. Schmidt H, Maier E, Karch H, Benz R. Pore-forming properties of the plasmid-encoded hemolysin of enterohemorrhagic Escherichia coli O157:H7. European journal of biochemistry / FEBS. 1996; 241:594–601. [PubMed: 8917461]
58. Lear JD, Furblur UG, Lally ET, Tanaka JC. Actinobacillus actinomycetemcomitans leukotoxin forms large conductance, voltage-gated ion channels when incorporated into planar lipid bilayers. Biochimica et biophysica acta. 1995; 1238:34–41. [PubMed: 7544624]
59. Brown AC, Boesze-Battaglia K, Du Y, Stefano FP, Kieba IR, Epand RF, Kakalis L, Yeagle PL, Epand RM, Lally ET. Aggregatibacter actinomycetemcomitans leukotoxin cytotoxicity occurs through bilayer destabilization. Cellular microbiology. 2012; 14:869–881. [PubMed: 22309134]
60. Walters MJ, Brown AC, Edrington TC, Baranwal S, Du Y, Lally ET, Boesze-Battaglia K. Membrane association and destabilization by Aggregatibacter actinomycetemcomitans leukotoxin requires changes in secondary structures. Molecular oral microbiology. 2013; 28:342–353. [PubMed: 23678967]
61. Bauer ME, Welch RA. Association of RTX toxins with erythrocytes. Infection and immunity. 1996; 64:4665–4672. [PubMed: 8890223]
62. Cortajarena AL, Goni FM, Ostolaza H. Glycophorin as a receptor for Escherichia coli alpha-hemolysin in erythrocytes. The Journal of biological chemistry. 2001; 276:12513–12519. [PubMed: 11134007]
63. Lally ET, Kieba IR, Sato A, Green CL, Rosenbloom J, Korostoff J, Wang JF, Shenker BJ, Ortlepp S, Robinson MK, Billings PC. RTX toxins recognize a beta2 integrin on the surface of human target cells. The Journal of biological chemistry. 1997; 272:30463–30469. [PubMed: 9374538]
64. Valeva A, Walev I, Kemmer H, Weis S, Siegel I, Boukhallouk F, Wassenaar TM, Chavakis T, Bhakdi S. Binding of Escherichia coli hemolysin and activation of the target cells is not receptor-dependent. The Journal of biological chemistry. 2005; 280:36657–36663. [PubMed: 16131494]
65. Benz R. Porin from bacterial and mitochondrial outer membranes. CRC critical reviews in biochemistry. 1985; 19:145–190. [PubMed: 2415299]
66. Belmonte G, Cescatti L, Ferrari B, Nicolussi T, Ropele M, Menestrina G. Pore formation by Staphylococcus aureus alpha-toxin in lipid bilayers. Dependence upon temperature and toxin concentration. European biophysics journal : EBJ. 1987; 14:349–358. [PubMed: 2439323]
67. Chakraborty T, Schmid A, Notermans S, Benz R. Aerolysin of Aeromonas sobria: evidence for formation of ion-permeable channels and comparison with alpha-toxin of Staphylococcus aureus. Infection and immunity. 1990; 58:2127–2132. [PubMed: 1694819]
68. Bhakdi S, Mackman N, Nicaud JM, Holland IB. Escherichia coli hemolysin may damage target cell membranes by generating transmembrane pores. Infection and immunity. 1986; 52:63–69. [PubMed: 3514465]
69. Barcena-Uribarri I, Thein M, Barbot M, Sans-Serramitjana E, Bonde M, Mentele R, Lottspeich F, Bergstrom S, Benz R. Study of the Protein Complex, Pore Diameter, and Pore-forming Activity of the Borrelia burgdorferi P13 Porin. The Journal of biological chemistry. 2014; 289:18614–18624. [PubMed: 24825899]
70. Barcena-Uribarri I, Thein M, Maier E, Bonde M, Bergstrom S, Benz R. Use of nonelectrolytes reveals the channel size and oligomeric constitution of the Borrelia burgdorferi P66 porin. PloS one. 2013; 8:e78272. [PubMed: 24223145]
71. Ternovsky VI, Okada Y, Sabirov RZ. Sizing the pore of the volume-sensitive anion channel by differential polymer partitioning. FEBS letters. 2004; 576:433–436. [PubMed: 15498575]
72. Ropele M, Menestrina G. Electrical properties and molecular architecture of the channel formed by Escherichia coli hemolysin in planar lipid membranes. Biochimica et biophysica acta. 1989; 985:9–18. [PubMed: 2477066]
73. Mafakheri S, Barcena-Uribarri I, Abdali N, Jones AL, Sutcliffe IC, Benz R. Discovery of a cell wall porin in the mycolic-acid-containing actinomycete Dietzia maris DSM 43672. The FEBS journal. 2014; 281:2030–2041. [PubMed: 24707935]

74. Trias J, Benz R. Characterization of the channel formed by the mycobacterial porin in lipid bilayer membranes. Demonstration of voltage gating and of negative point charges at the channel mouth. The Journal of biological chemistry. 1993; 268:6234–6240. [PubMed: 7681063]

75. Trias J, Benz R. Permeability of the cell wall of Mycobacterium smegmatis. Molecular microbiology. 1994; 14:283–290. [PubMed: 7830572]

76. Menestrina G, Antolini R. Ion transport through hemocyanin channels in oxidized cholesterol artificial bilayer membranes. Biochimica et biophysica acta. 1981; 643:616–625. [PubMed: 6264956]

77. Nelson AP, McQuarrie DA. The effect of discrete charges on the electrical properties of a membrane. I. Journal of theoretical biology. 1975; 55:13–2. [PubMed: 1586]

78. Ehrmann IE, Gray MC, Gordon VM, Gray LS, Hewlett EL. Hemolytic activity of adenylate cyclase toxin from Bordetella pertussis. FEBS letters. 1991; 278:79–83. [PubMed: 1993477]

Highlights

- RtxA toxin is the major virulence factor of pediatric pathogen *Kingella kingae*.
- This is the first study to characterize *K. kingae* RtxA pore forming activity in planar lipid bilayers.
- RtxA forms cation-selective pores in artificial lipid membranes with an apparent pore diameter of 1.9 nm.
- RtxA is able to form large pores in cell membranes resulting in cation flux.

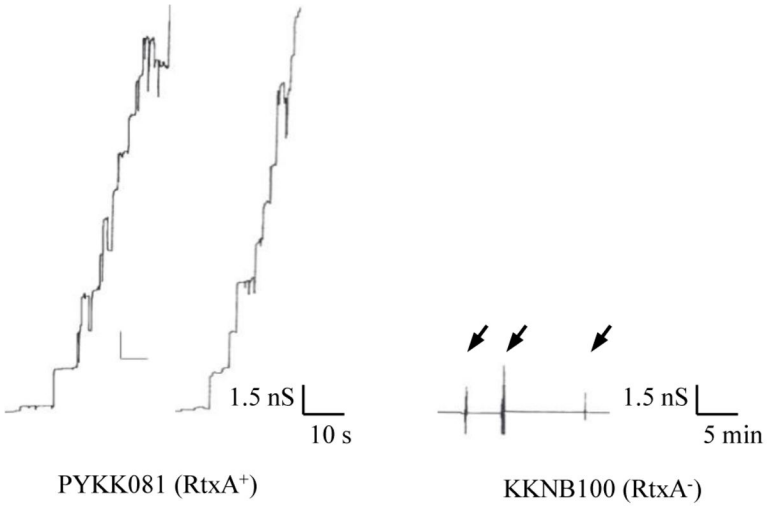

Fig. 1. Pore forming activity of the supernatants of *K. kingae* strain PYKK081 and the RtxA-deficient strain KKNB100

Left panel: Single channel recording of an asolectin/*n*-decane membrane in the presence of 100μl supernatant from strain PYKK081. The aqueous phase contained 1 M KCl, 10 mM MES, pH 6.0. The applied membrane potential was 20 mV.

Right panel: Single-channel recording of an asolectin/*n*-decane membrane in the presence of increasing amounts of the supernatant from strain KKNB100. The arrows indicate successive additions of 200 μl supernatants to the aqueous phase bathing the membrane. The aqueous phase contained 1 M KCl, 10 mM MES, pH 6.0. No current fluctuations were observed under these conditions

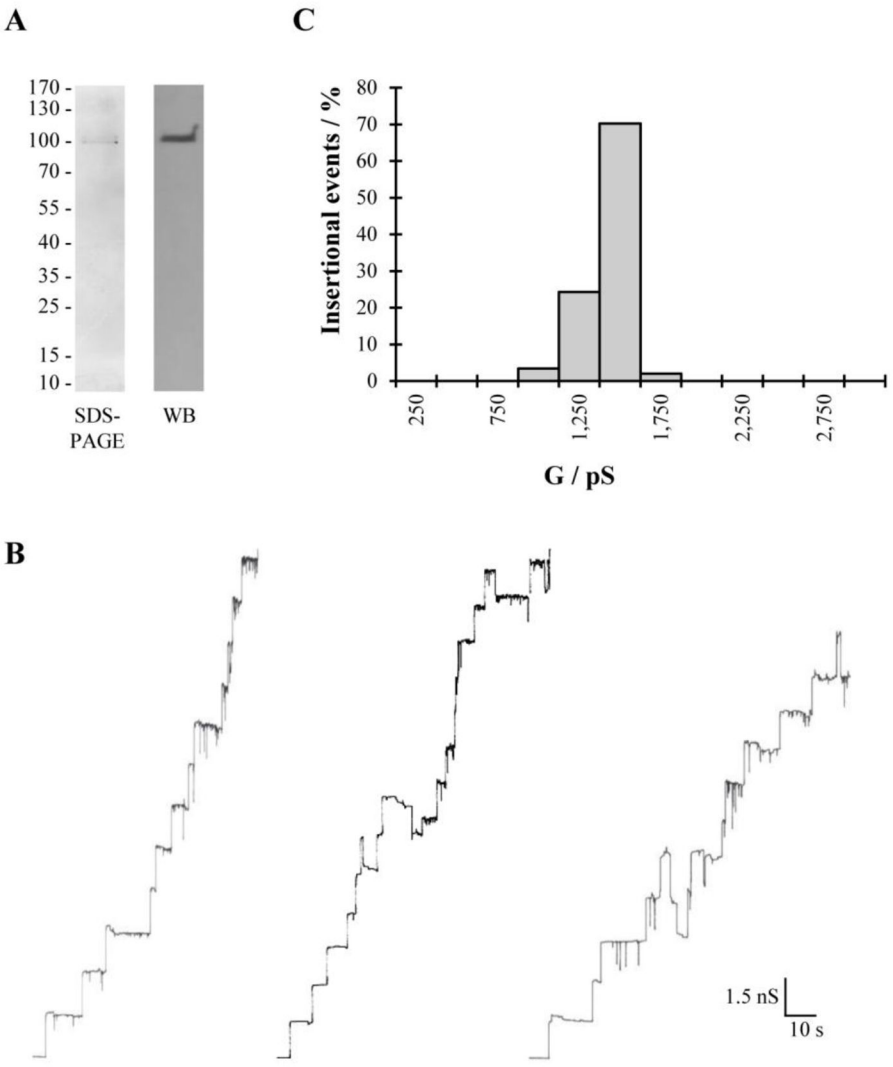

Fig. 2. Purification and pore forming activity of *K. kingae* RtxA

(A) SDS-PAGE and Western blot analysis of purified RtxA. The only band of approximately 100 kDa was detected on SDS-PAGE in the purified active sample. This protein was recognized by 10A7D7, the specific anti-RtxA antibody. (B) Single channel insertions of purified RtxA in 3 independent newly formed asolectin/n-decane membranes bathed in 1M KCl, 20 mV applied voltage and (C) Histogram summarizing the pore forming activity of the sample. The predominant single-channel conductance was 1.5 nS for 148 single-channel events.

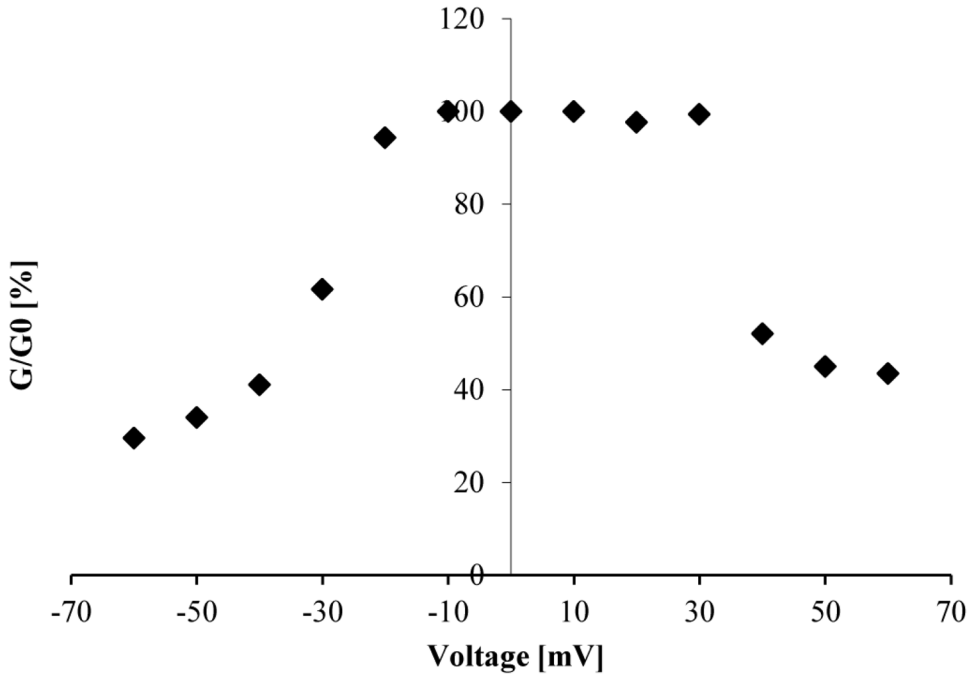

Fig. 3. Voltage-dependent gating of *K. kingae* RtxA

Increasing positive and negative voltages were applied to RtxA containing membrane to study its gating behavior. The initial value of the conductance (Go) obtained immediately after the onset of the voltage was divided by conductance of the membrane once the opening and closing of channels reached equilibrium after the membrane current decay due to the voltage step (G). Go/G (%) was calculated individually for each applied voltage. The results depicted in this figure are the average values obtained from three independent membranes subjected to positive and negative voltages in increasing order.

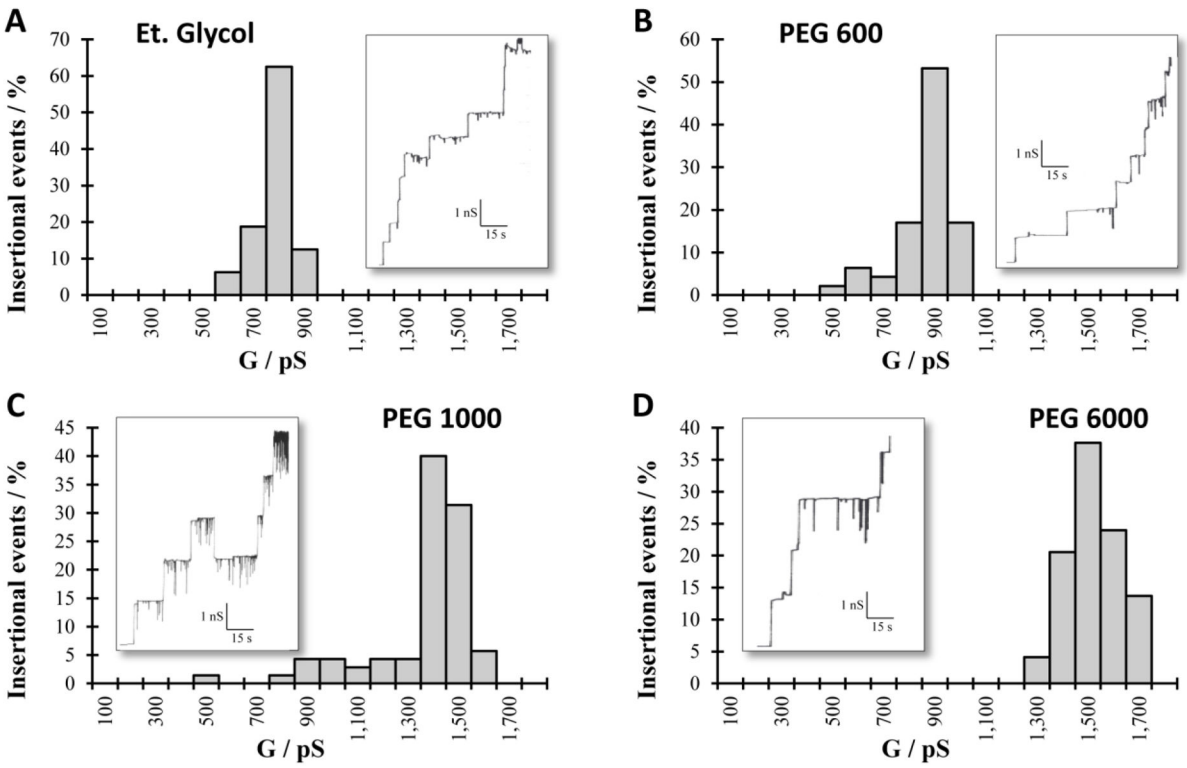

Fig. 4. Single channel conductance of *K. kingae* RtxA in 1 M KCl solution containing specific 20% NEs

Histogram and single channel insertions record (embedded panel) for RtxA in 1M KCl plus 20% (w\v) of A) ethylene glycol B) PEG 600 C) PEG 1000 and D) PEG 6000. The probability for the occurrence of certain conductance levels in percent were calculated from at least 50 insertions and the conductance (G) is expressed in Pico Siemens (pS). The applied voltage was 20 mV in all experiments.

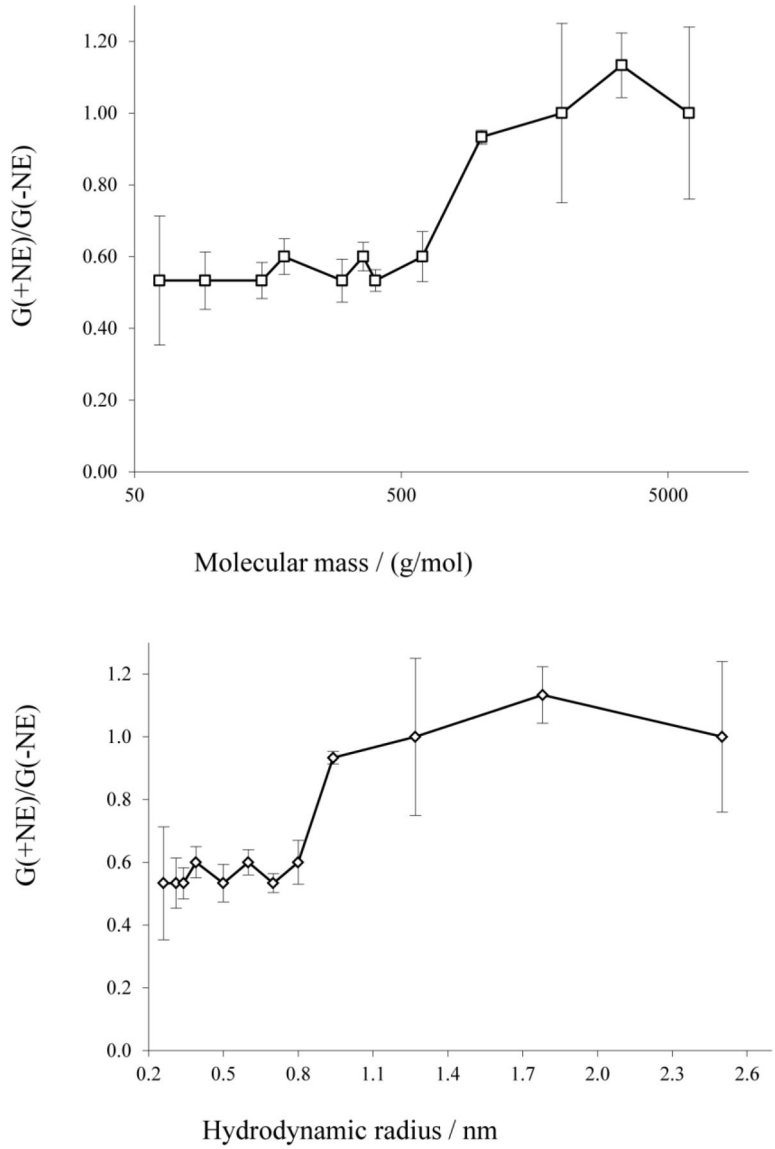

Fig. 5. *K. kingae* RtxA single-channel conductance dependence on the (A) molecular mass and (B) the hydrodynamic radius of NEs

G(+NE)/G(−NE) is the ratio of the single-channel channel conductance in the presence of NEs to that in the absence of NEs. Molecular masses and hydrodynamic radii of NEs are presented in Table 3. The bars indicate the standard deviation.

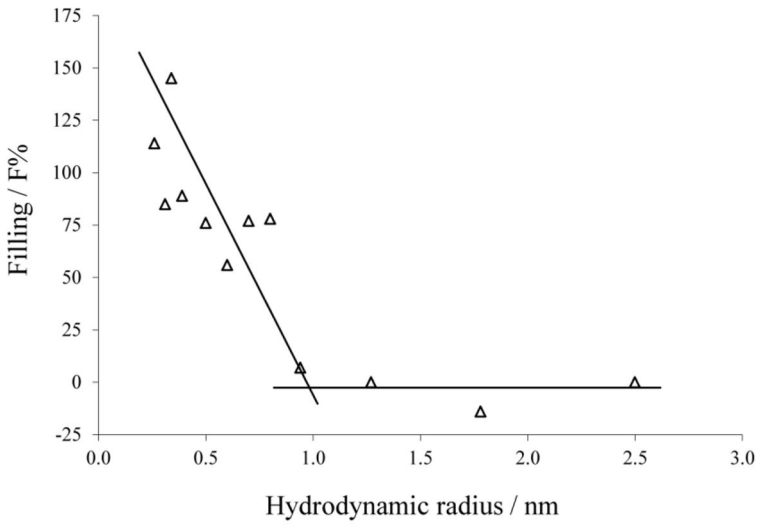

Fig. 6. *K. kingae* RtxA channel filling (F%) dependence on the NEs hydrodynamic radii

F% for each NE was calculated according to Eq. 2. Lines are best fits to the experimental points. The horizontal lines connect the points derived from measurements in the presence of PEG 1000, PEG 2000, PEG 3350, and PEG 6000. The other line regression was used to describe the points for the NEs with radii ranging from 0.26 nm to 0.8 nm (ethylenglycol, glycerol, arabinose, sorbitol, PEG 200, PEG 300, PEG 400, and PEG 600). Hydrodynamic radii of the NEs are presented in Table 3.

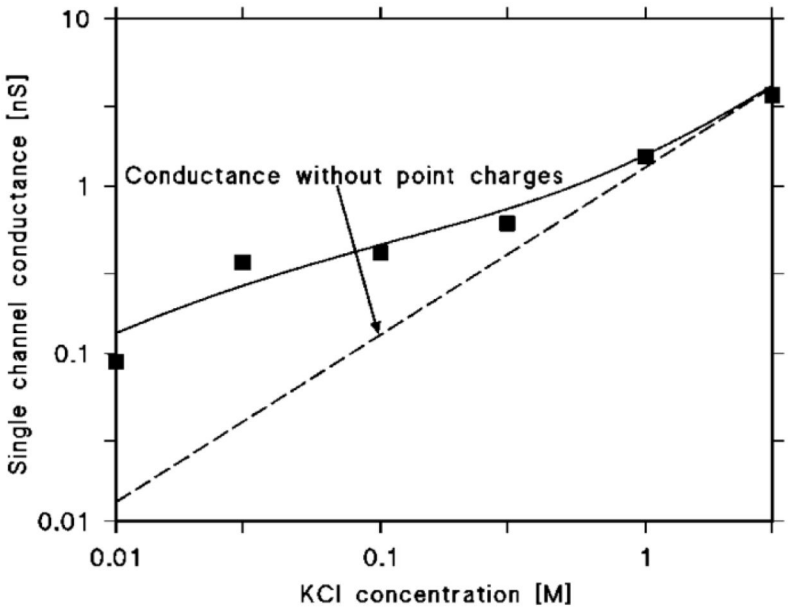

Fig. 7. Single channel conductance of *K. kingae* RtxA as a function of the KCl concentration

The squares represent the conductance of RtxA in different concentrations of KCl in the solution. The solid line represents the fit of the single channel conductance as described in the methods [76, 77] and assuming the presence of 2 negative charges ($q=-3.2\cdot10^{-19}$ As) at both sides of the membrane and a channel radius of 0.9 nm. The dashed line corresponds to the single channel conductance of the RtxA channel in the absence of point charges and represents a linear function between the channel conductance and the salt concentration.

Table 1

Single channel conductance of *K. kingae* RtxA in solutions of different electrolytes.

Salt	Concentration (M)	G ± SD (nS)
KCl	0.01	0.09 ± 0.01
	0.03	0.35 ± 0.04
	0.1	0.4 ± 0.03
	0.3	0.6 ± 0.05
	1	1.5 ± 0.14
	3	3.5 ± 0.26
LiCl	1	0.7 ± 0.05
KAc	1	1.3 ± 0.06

The RtxA conductance (G) in each salt solution was taken from the highest probability for the occurrence of conductance observed in a Gaussian distribution of single channel conductance. To analyze the conductance in each case at least 50 channels were reconstituted in asolectin membranes at 20 mV voltage. The solutions used were unbuffered with pH close 6.0. The pH of KAc was adjusted to pH 7.0 using acetic acid.

Table 2

Zero-current membrane potentials of 1% asolectin/n-decane membranes in the presence of *K. kingae* RtxA measured for 5-fold gradients of different salts (100 mM versus 500 mM).

Salt	V_m ± SD (mV)	P_{cation}/P_{anion}
KCl	+19.9 ± 1.49	3.49
LiCl	+16.59 ± 1.49	2.76
KAc	+21.03 ± 0.83	3.79

The zero-current membrane potentials (V_m) were defined as the difference between the potential at the dilute side (measuring electrode) and the potential at the concentrated side. The aqueous salt solutions were used unbuffered and had a pH around pH 6. The pH of the KAc solution was adjusted to 7.0 with acetic acid. The permeability ratio P_{cation}/P_{anion} was calculated using the Goldman-Hodgkin-Katz equation [37] using the average membrane potential of at least 3 individual experiments.

Table 3

Single channel conductance of *K. kingae* RtxA in presence of different NEs.

Nonelectrolyte	*r* (*nm*)	Mr (g/mol)	χ (mS/cm)	*G* ± SD (*nS*)	F	F%
None	-	-	110.3	1.50 ± 0.14	-	-
Et. glycol	0.26	62	57.2	0.80 ± 0.18	0.94	114.63
Glycerol	0.31	92	49.1	0.80 ± 0.08	0.70	85.37
Arabinose	0.34	150	63.7	0.80 ± 0.05	1.20	145.46
Sorbitol	0.39	182	57.8	0.90 ± 0.05	0.73	89.26
PEG 200	0.50	300	46.1	0.80 ± 0.06	0.63	76.41
PEG 300	0.60	360	45.5	0.90 ± 0.04	0.47	56.93
PEG 400	0.70	400	46.4	0.80 ± 0.03	0.64	77.27
PEG 600	0.80	600	54.1	0.90 ± 0.07	0.64	78.05
PEG 1000	0.94	1000	49.5	1.40 ± 0.01	0.06	7.07
PEG 2000	1.27	2000	56.5	1.50 ± 0.25	0.00	0.00
PEG 3350	1.78	3350	56.4	1.70 ± 0.09	−0.12	−14.97
PEG 6000	2.5	6000	50.5	1.5 ± 0.24	0.00	0.00

The single channel experiments were performed in 1 M KCl and 20% (w/v) of the corresponding NE. The hydrodynamic radius (r) and the molecular mass (Mr) of the NEs as well as the conductivity (χ) of the 1M KCl solutions containing 20% of different NEs were taken from previous publications [40–42]. The single channel conductance (G) and its standard deviation (SD) were calculated from at least 50 conductance steps. Channel filling (F) and percentage of channel filling (%F) were calculated as described in the methods section. V_m=20 mV; T=20 °C. Et. Glycol: ethylene glycol.

Table 4

Comparison of the pore forming properties of different RTX toxins in lipid bilayer membranes.

Toxin	SCC	IS	VG	PD
RtxA *K. kingae*	400 pS (0.1 M KCl)*	Cation select P_K/P_{Cl} = 3.5*	30–40 mV*	1.9 nm (a)*
HylA *E. coli*	500 pS (0.15 M KCl) [46]	Cation select [46] P_K/P_{Cl} = 9	<100 mV [46]	1.4–3 nm [68] (b)
EHEC-Hly *E. coli* EHEC	500 pS (0.15 M KCl) [57]	Cation select [57] P_K/P_{Cl} = 13	No data	2.6 nm [57] (b,c)
ApxI *A. pleuropneumoniae*	540 pS (0.15 M KCl) [56]	Cation select [56] P_K/P_{Cl} = 5.7	No data	2.4 nm [56] (c)
ApxII *A. pleuropneumoniae*	620 pS (0.15 M KCl) [56]	Cation select [56] P_K/P_{Cl} = No data	No data	2.5 nm [56] (c)
ApxIII *A. pleuropneumoniae*	95 pS (0.15 M KCl) [56]	Cation select [56] P_K/P_{Cl} = 9.6	No data	1.8 nm [56] (c)
CyaA *B. pertussis*	27 pS (1M KCl) [29]	Cation select [29] P_K/P_{Cl}= 9–11	No data	0.6–0.8 nm [29, 78] (b,c)
Rtx *P. vulgaris*	500 pS (0.15 M KCl) [45]	Cation select [45] (P_K/P_{Cl} = 9.5)	≥ 40 mV [45]	> 1 nm [45] (c)
Rtx *M. morganii*	500 pS (0.15 M KCl) [45]	Cation select [45] (P_K/P_{Cl} = 10)	≥ 40 mV [45]	> 1 nm [45] (c)
Lkt *A. actinomycetemcomitans*	406 pS (0.14 M NaCl, 0.01 M $CaCl_2$) [58]	No data	No data	No data

The biophysical properties such as single channel conductance (SCC), ion selectivity (IS), voltage-dependent gating (VG), and the pore diameter (PD) were compared for several RTX toxins. The references to the original studies are included, while the results included in this study are marked with an asterisk (*). The SCC showed in the Table refers to the open state of the pore with higher conductance. The P_K/P_{Cl} values shown in the Table are referred to experiments performed in KCl solutions. The values for the pore diameter were obtained using the following methods; (a) partition experiments with NEs, (b) Osmotic protection experiments and (c) mobility sequence of different cations.